Desalination and Water Treatment

ISSN: 1944-3994 (Print) 1944-3986 (Online) Journal homepage: http://www.tandfonline.com/loi/tdwt20

Photocatalytic degradation of methylene blue and methyl orange in a Zn(II)-based Metal–Organic Framework

Chong-Chen Wang, Yan-Qiu Zhang, Tian Zhu, Peng Wang & Shi-Jie Gao

To cite this article: Chong-Chen Wang, Yan-Qiu Zhang, Tian Zhu, Peng Wang & Shi-Jie Gao (2016) Photocatalytic degradation of methylene blue and methyl orange in a Zn(II)-based Metal–Organic Framework, Desalination and Water Treatment, 57:38, 17844-17851, DOI: 10.1080/19443994.2015.1088807

To link to this article: http://dx.doi.org/10.1080/19443994.2015.1088807

Desalination and Water Treatment
www.deswater.com
doi: 10.1080/19443994.2015.1088807

57 (2016) 17844–17851
August

Taylor & Francis
Taylor & Francis Group

Photocatalytic degradation of methylene blue and methyl orange in a Zn(II)-based Metal–Organic Framework

Chong-Chen Wang[a,b,*], Yan-Qiu Zhang[a], Tian Zhu[a], Peng Wang[a], Shi-Jie Gao[a]

[a]*Key Laboratory of Urban Stormwater System and Water Environment (Ministry of Education), Beijing University of Civil Engineering and Architecture, Beijing 100044, China, Tel./Fax: +86 10 6832 2124; emails: chongchenwang@126.com (C.-C. Wang), candy7zyq@163.com (Y.-Q. Zhang), 1194947305@qq.com (T. Zhu), wangpeng@bucea.edu.cn (P. Wang), gaoshijie@bucea.edu.cn (S.-J. Gao)*
[b]*Beijing Engineering Research Center of Sustainable Urban Sewage System Construction and Risk Control, Beijing University of Civil Engineering and Architecture, Beijing 100044, China*

Received 6 February 2015; Accepted 20 August 2015

ABSTRACT

A novel 3D Zn(II)-based metal-organic framework $[Zn_2(odpt)(bpy)(H_2O)](bpy)_{0.5}$ (**1**) (H_4odpt = 4,4′-oxidiphthalic acid, bpy = 4,4′-bipydine) has been hydrothermally synthesized, and characterized by the single-crystal X-ray diffraction, Fourier transform infrared spectroscopy, UV–vis diffuse spectrum, and thermal gravimetric analysis. Compound **1** shows highly efficient photocatalytic activity on the degradation of individual methylene blue (MB) and methyl orange (MO), while exhibits a preferential photocatalytic degradation of MO in the MO/MB mixture under UV light irradiation. The possible photocatalytic mechanism was proposed, which was confirmed by trapping experiments of radicals via the addition isopropanol as radical scavenger, and compound **1** exhibits excellent recyclability and stability, which can achieve good degradation efficiency to MB for five runs.

Keywords: Metal-organic framework; Photocatalytic degradation; Diffuse reflectance; Photocatalytic mechanism

1. Introduction

The increase in the amount of wastewater containing organic dyes led to a big challenge all over the world. Organic dye molecules usually involve one or more benzene rings which are hard to be degraded by conventional chemical and biological methods [1]. Photocatalytic degradation of organic dyes is really of considerable attention due to increasing strict standards of controlling environmental pollution prior to discharging into the environment. Over the past decades, heterogeneous photocatalysis using semiconductor catalysts such as TiO_2, ZnO, Fe_2O_3, CdS, GaP, and ZnS attracted a lot of attention due to its universal applications, especially in direct utilization of solar energy. The heterogeneous photocatalysis based on typical semiconductor catalysts possesses some significant advantages, but also faces some unavoidable challenges and drawbacks [1]. It is a hot topic in some research fields like material science, green chemistry, and environmental science to look for new photocatalysts with improved performances.

Metal–organic frameworks (MOFs), a class of newly developed inorganic–organic hybrid materials, have attracted much attention [2], due to their diverse and easily tailored structures [3–6], as well as various

*Corresponding author.

potential applications, like catalysis [7,8], separation [9], gas storage [10,11], carbon dioxide capture [12], and so on. Recent researches indeed demonstrated that some MOFs materials are a new class of photocatalysts usable in photocatalytic degradation of organic pollutants under UV/visible/UV–visible irradiation [1,3,4,13–17]. Based on the richness of metal nodes and organic linkers, as well as the controllability of synthesis, it is easy to construct MOFs with tailorable capacity to absorb light, thereby initiating desirable photocatalytic decomposition of organic pollutants in MOFs [1]. In contrast to the conventional photocatalysts of metal oxides and sulfides, the study of MOFs' utilization as heterogeneous photocatalysts thus has a bright future, in spite of not being so widely explored to date.

With this study, a Zn(II)-based metal–organic framework $[Zn_2(odpt)(bpy)(H_2O)](bpy)_{0.5}$ (**1**) (H_4odpt = 4,4′-oxidiphthalic acid, bpy = 4,4′-bipydine) was hydrothermally synthesized and used as photocatalyst to decompose two typical organic dyes: methylene blue (MB), a heterocyclic aromatic dye, and methyl orange (MO), a stable azo dye with resisting to biodegradation [18–26], and even their mixture. The results revealed that compound **1** exhibits highly efficient activity to degrade individual MO and MB, and shows preferential photocatalytic degradation of MO in the MO/MB mixture. The possible mechanism was also proposed to clarify the degradation of organic dyes in the presence of **1.**

2. Experimental

2.1. Synthesis of the photocatalysts

All chemicals were commercially available reagent grade, and used without further purification. A mixture of $ZnCl_2$ (0.3 mmol, 0.0409 g), H_4odpt (0.3 mmol, 0.1075 g), and 4,4′-bpy (0.6 mmol, 0.0937 g) with a molar ratio of 1:1:2 was sealed in a 25-mL Teflon-lined stainless steel Parr bomb containing deionized H_2O (20 mL), heated at 160°C for 72 h, and then cooled down to room temperature [27]. Light brown rod-like crystals were isolated and washed with deionized water and ethanol (yield 68% based on $ZnCl_2$). Anal. Calcd. for **1**, $C_{31}H_{20}N_3O_{10}Zn_2$: C, 51.3; N, 5.8; H, 2.8. Found: C, 51.4; N, 5.8; H, 2.8·IR (KBr)/cm^{-1}: 3,329, 3,052, 1,598, 1,557, 1,490, 1,416, 1,362, 1,230, 1,254, 1,153, 1,136, 1,070, 1,046, 1,013, 968, 930, 905, 859, 838, 791, 778, 725, 687, 664, 642, 624, 611, 587, 509, 464.

2.2. Characterizations

CNH elemental analyses were conducted using an Elementar Vario EL-III instrument. Fourier transform infrared spectroscopy (FTIR) spectra, in the region (400–4,000 cm^{-1}), were recorded on a Nicolet 6700 Fourier Transform infrared spectrophotometer. X-ray single-crystal data collection for **1** was performed with Bruker Smart 1000 CCD area detector diffractometer with a graphite-monochromatized MoK_α radiation (λ = 0.71073 Å) using φ-ω mode at 298(2) K. UV–vis diffuse reflectance spectra of solid samples were measured from 200 to 1,200 nm by PerkinElmer Lamda 650S spectrophotometer, in which barium sulfate ($BaSO_4$) was used as the reference with 100% reflectance. Thermal gravimetric analysis (TGA) was performed from room temperature to 900°C in an air stream at a rate of 10°C min^{-1} on a TA SDT Q600 TGA system using a-Al_2O_3 as reference material.

2.3. Photocatalytic degradation

The photocatalytic activity of **1** as photocatalysts was evaluated by the photodegradation of MB, MO, and the mixture of MB and MO dyes under 500 W Hg lamp irradiation at room temperature in photocatalytic assessment system (Beijing Aulight Co., Ltd). The distance between the light source and the beaker containing reaction mixture was fixed at 5 cm. Fifty mg of **1** was put into 200 mL of MB (10 mg/L), MO (10 mg/L), or mixture of MO and MB (10 mg/L for MO and MB, respectively) aqueous solution in a 300-mL flask. Prior to irradiation, the suspension was magnetically stirred in dark for 120 min to ensure the establishment of an adsorption/desorption equilibrium. During the photodegradation reaction, stirring was maintained to keep the mixture in suspension. One milliliter sample was extracted at regular intervals using 0.45 μm syringe filter (Shanghai Troody) for analysis. A Laspec Alpha-1860 spectrometer was used to monitor the changes of the dye absorbance in the range of 200–800 nm in a **1**-cm path length spectrometric quartz cell. The MB and MO concentration was estimated by the absorbance at 664 and 463 nm, respectively [17]. In order to test the effect of pH on photocatalytic degradation, the initial pH of MB solution was adjusted from 2.0 to 12.0 with HCl (1.0 M) and NaOH (1.0 M), respectively, to test the degradation efficiency of MB on **1**.

3. Results and discussion

3.1. Characterization

Single-crystal X-ray diffraction data revealed that the formula of $[Zn_2(odpt)(bpy)(H_2O)](bpy)_{0.5}$ was $C_{31}H_{20}N_3O_{10}Zn_2$ with FW = 725.24, monoclinic, space group P2(1)/n, a = 10.9411(8) Å, b = 15.0912(13) Å,

c = 16.5165(16) Å, α = 90°, β = 92.0100(10)°, γ = 90°, V = 2725.4(4) Å^3, Z = 4, D_c = 1.767 Mg/m^3, μ = 1.831 mm^{-1}, a total of 13,436 reflections were collected, 4,773 of which were unique (R_{int} = 0.0409), final R_1 = 0.0363 for I > 2σ(I), wR_2 = 0.0845 for all data, GOOF = 1.029. Compound **1** consists of a network of distorted tetrahedral Zn1O$_3$N units and distorted octahedral Zn2O$_5$N units completed by bpy, odpt^{4-}, and water molecule, with discrete bpy molecules lying in the channels of the 3D framework, as shown in Fig. 1(a) and (b). The Zn(II) centers are linked into 2D sheet along *a*-axis, as shown in Fig. 1(c), and the bidentate bpy further joins the 2D sheets into 3D framework, as illustrated in Fig. 1(d), in which the hydrogen bonding interactions enhanced the structure of this 3D framework. TGA result shows a weight loss of 4.14% around 250℃ corresponding to the release of coordinated water and free 4,4-bipy molecules (calcd. 3.56%) and further decomposition occurred at 320℃. All these data agreed well with the previously reported ones by Chu and coworkers [27].

In order to investigate the conductivity of **1**, the measurement of UV–vis diffuse reflectivity for a powder sample was used to obtain its optical band gap E_g. The band gap E_g was determined as the intersection point between the energy axis and the line extrapolated from the linear portion of the absorption edge in a plot of Kubelka–Munk function F against energy E. Kubelka–Munk function, $F = (1 - R)^2/2R$, was converted from the recorded diffuse reflectance data, where R is the reflectance of an infinitely thick layer at a given wavelength [28,29]. The F vs. E plots for the compound **1** are shown in Fig. 2, where steep absorption edges are displayed and the E_g of **1** can be assessed at 3.6 eV, indicating that **1** showed selective absorption in the ultraviolet spectrum region [3,4].

3.2. Photocatalytic degradation of individual MO and MB

It is well known that MOFs have already been used for new photocatalytic materials in view of their potential applications in the degradation of organic

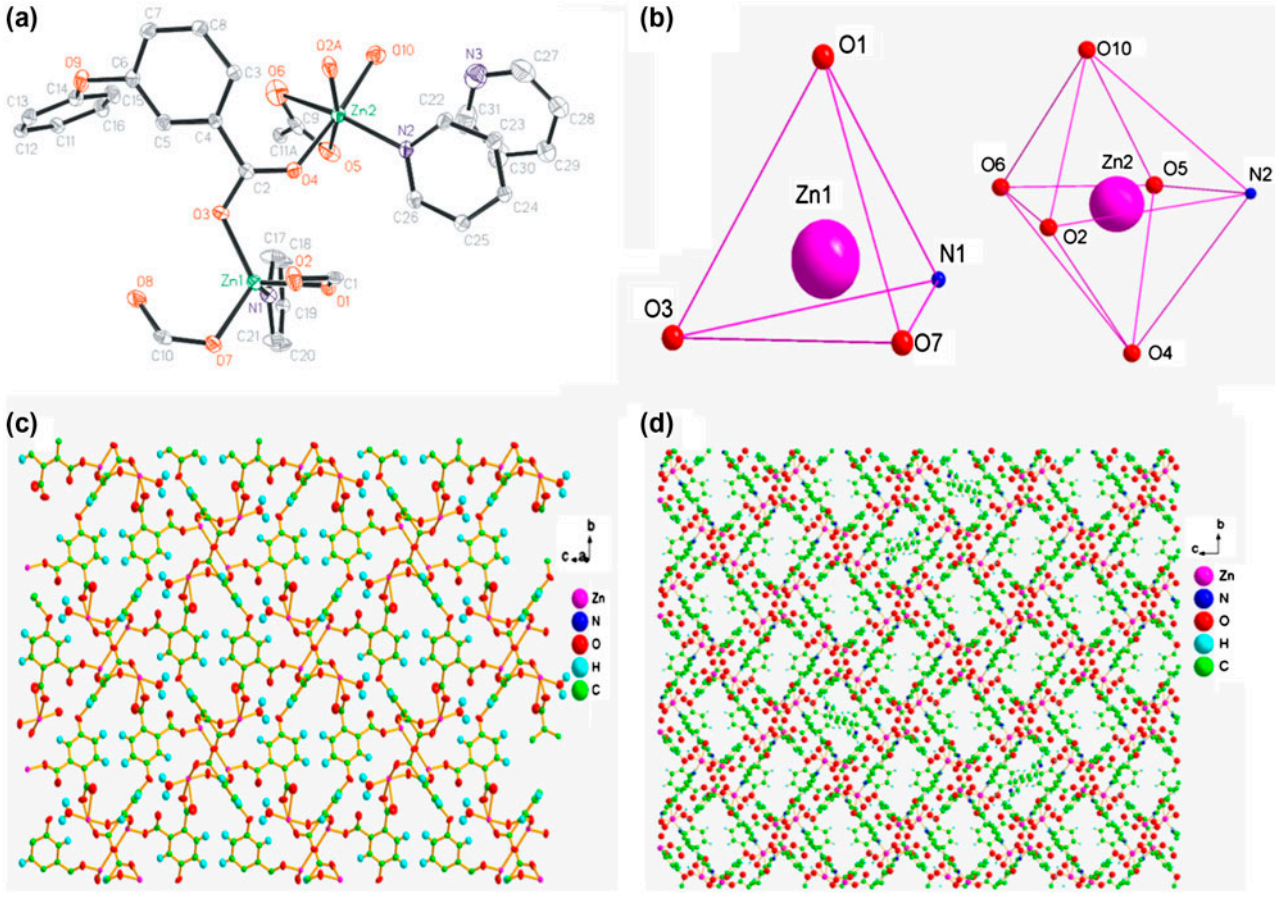

Fig. 1. (a) Asymmetric unit of [Zn$_2$(odpt)(bpy)(H$_2$O)](bpy)$_{0.5}$ (**1**), (b) Coordination environments around the Zn(II) atoms, (c) 2D sheet built from Zn(II) and odpt^{4-} along *a*-axis in complex **1,** and (d) 3D framework of **1** along *a*-axis.

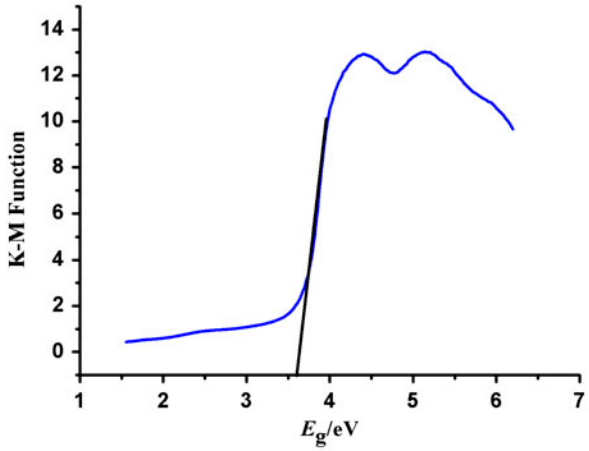

Fig. 2. Kubelka–Munk—transformed diffuse reflectance spectra of compound **1.**

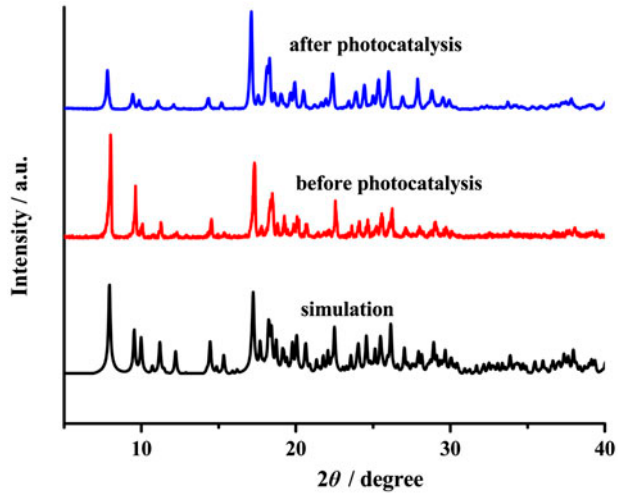

Fig. 3. PXRD patterns of compound 1 before and after photocatalytic reaction and the simulated XRD pattern from single crystal structure of compound **1.**

pollutants [1,3,4]. The photocatalytic performances of compound **1** for the photodegradation of individual MB and MO were carried out under UV irradiation. In order to confirm the powder purities of compound **1** used in this experiment, powder X-ray diffraction was conducted, and the results revealed that the powder X-ray patterns match well with the corresponding simulated patterns from the single X-ray crystal structure data. The comparison between powder X-ray patterns and simulated patterns of compound **1** was illustrated in Fig. 3. Control experiments on photodegradation of MB and MO were performed. Fig. 4 illustrated the efficiencies of MB and MO's degradation after the dark adsorption equilibrium achieved according to the previously reported reference [17]. The photocatalytic activity of **1** as photocatalyst was monitored by measuring the maximum absorbance intensity at $\lambda = 463$ and 664 nm characteristics of the targets MO and MB [1,4].

It can be seen that the photocatalytic activities of MB degradation increased from 27.5% (control experiment without **1** photocatalyst) to 90.9% under UV light irradiation within 120 min, and the MO degradation efficiency increased from 24.0% (without **1** photocatalyst) to 91.7% under the same conditions up to 40 min (Fig. 4), which was comparable to other reported MOFs [1,4,17]. Additionally, both the photodegradation reactions of MB and MO in **1** photocatalyst followed pseudo-first-order kinetics model with $R^2 = 0.954$ and $R^2 = 0.959$, respectively, as evidenced by the linear plot of ln (C/C_0) vs. reaction time t. The pseudo-first-order rate constants for the photocatalytic degradation of MB and MO in **1** photocatalyst were 0.019 and 0.0605 min^{-1}, respectively. As seen from Fig. 5(a) and

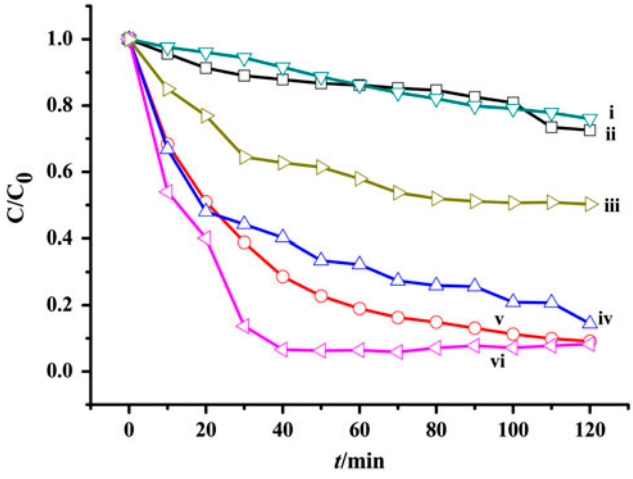

Fig. 4. Plots of concentration vs. irradiation time for MO and MB under irradiation with Hg lamplight ((i) and (ii): the control experiments for MO and MB degradation without any catalyst; (iii) and (iv): radicals trapping by IPA as scavenger in the system of photodegradation of MO and MB with **1** under UV light irradiation; e and vi: photocatalytic decomposition of MB and MO solution under UV with **1**).

(b), when the simulated wastewater samples of MB and MO were irradiated under UV light, the maximum absorption peaks of MB and MO decreased obviously with the reaction time in the presence of **1**. Furthermore, no other new peaks are observed in Fig. 5(a) and (b), indicating that no new pollutants occurred during the process of degradation.

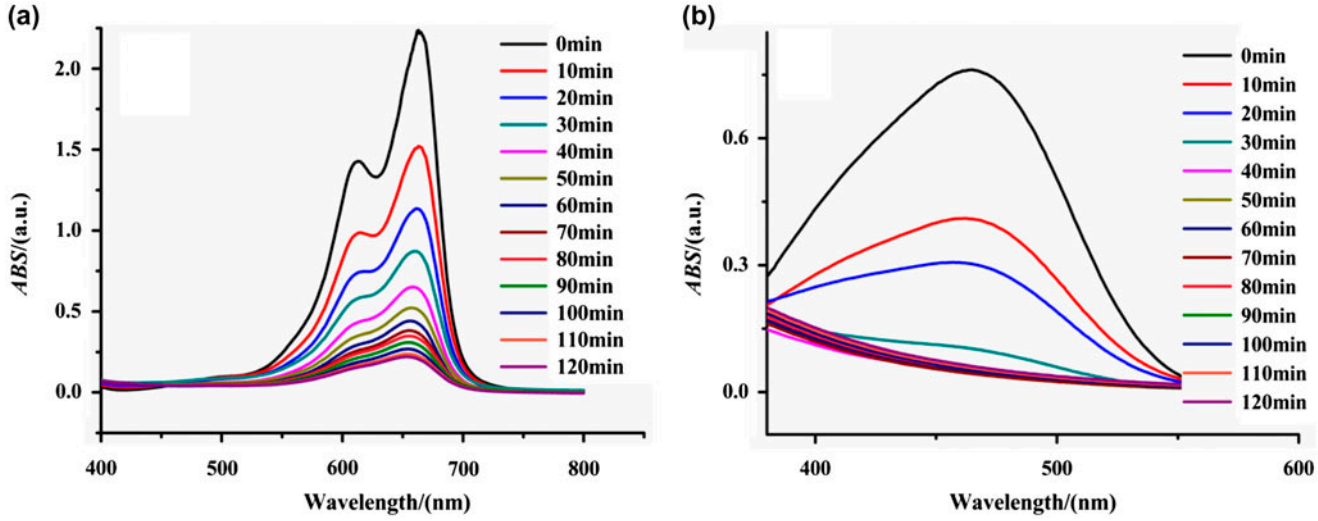

Fig. 5. UV–vis absorption spectra of the MB (a) and MO (b) solution during the photocatalytic degradation under Hg lamplight irradiation in the presence of **1**.

3.3. *Photocatalytic degradation of the mixture of MO and MB*

Further investigation of photocatalytic degradation activity was conducted on the MB/MO mixture. After 10 min of UV irradiation, the intensity of UV absorption peak of MO was observed to decrease sharply (the calculated degradation percentage reaching 81.8%), while intensity of UV absorption peak of MB still remains high level (the calculated degradation percentage being 17.4%), as illustrated in Fig. 6(a) and (b). After subsequent UV irradiation up to 60 min, a rapid degradation percentage of MB was then observed to be 74.5%. Totally, a higher degradation rate can be observed for MO compared to MB in the MO/MB mixture. This difference implied that compound **1** exhibits a preferential photocatalytic degradation of MO in the MO/MB mixture. The lower degradation percentage of MB in MO/MB mixture than individual MB solution can be mainly associated with the occurrence of the MO competitive consumption of the oxidizing species as well as that the presence of N=N makes MO more reactive, while the

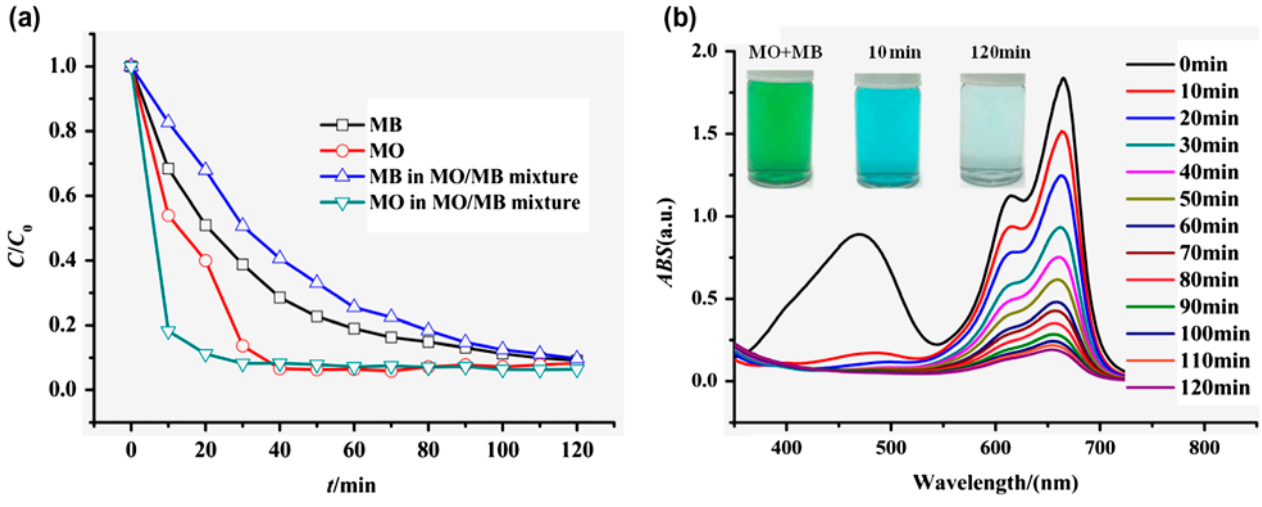

Fig. 6. (a) Plots of concentration vs. irradiation time for MO and MB after photocatalytic degradation under irradiation with Hg lamplight and (b) UV–vis absorption spectra of the MO and MB in MO/MB mixture solution during the photocatalytic degradation under Hg lamplight irradiation in the presence of **1**.

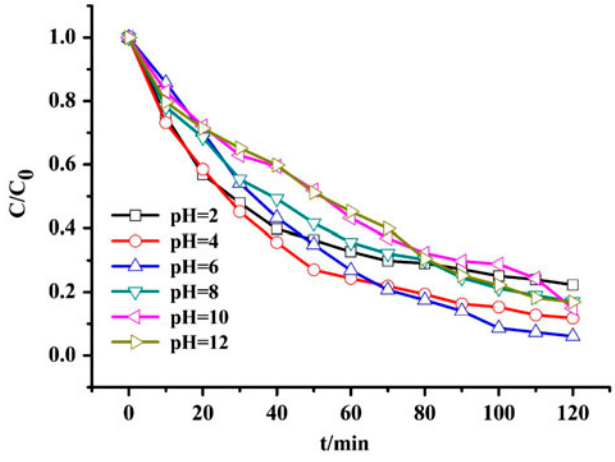

Fig. 7. Influence of pH on the photocatalytic degradation of MB in **1**. Experiment conditions: 0.05 g of **1**; 200 mL of MB solution with initial concentration of 10 mg/L.

presence of the $-CH_3$ group in MB makes it resist to photodegradation [30]. Similar preference in the degradation between MO and MB was reported previously for the mesoporous TiO_2 [31], $ZnO/ZnAl_2O_4$ powder [32], and $NiO\text{-}Bi_2O_3$ nanocomposite [33].

3.4. Effect of initial pH

The pH of the solution was an important parameter which may have influence on the photocatalytic degradation reactions [19]. Thus, the effect of initial pH on the degradation efficiency of MB in **1** was tested. The results revealed that **1** could work effectively over a wide pH range from 2.0 to 12.0, as illustrated in Fig. 7, which showed that **1** has great stability in strong acid and alkali.

3.5. Mechanism the photocatalytic degradation of MO and MB in 1

Generally, there is an electron transfer from the highest occupied molecular orbital (HOMO) to the lowest unoccupied molecular orbital (LUMO) in the presence of UV light. The HOMO is mainly contributed by O and/or N 2p bonding orbitals, and the LUMO is mainly contributed by empty M (like Zn) orbitals. With the irradiation of UV light, there is an electron transfer from the HOMO to LUMO. The electron of the excited state in the LUMO is usually very easily lost, while the HOMO strongly demands one electron to return to its stable state. Therefore, one electron is captured from water molecules, which is oxygenated into the ·OH active species. Then, the ·OH radicals can decompose MB or MO efficiently to complete the photocatalytic process. To understand the photocatalysis mechanisms of MOFs, the terminology of HOMO-LUMO gap rather than traditional semiconductor gap (CB-VB) is suggested to describe the discrete character of the light-induced transitions

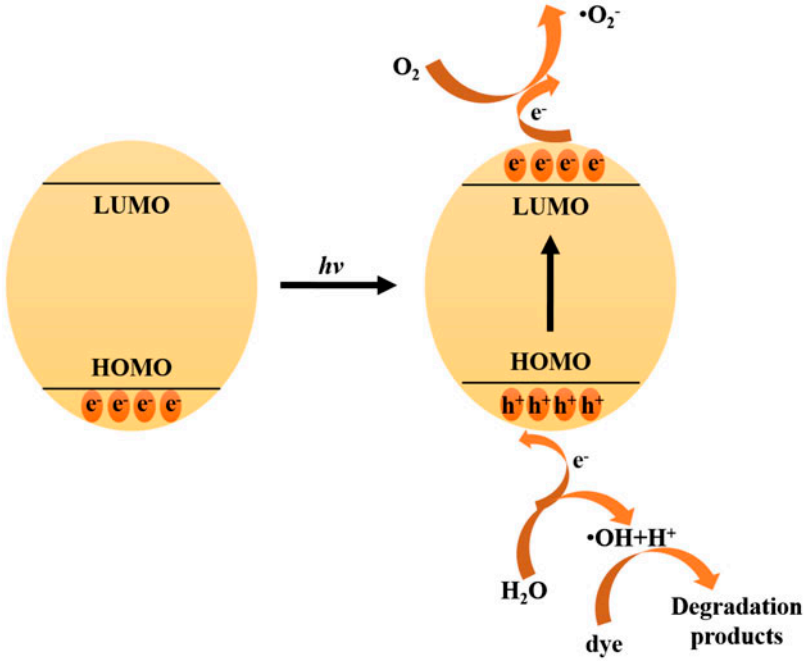

Fig. 8. A simplified model of photocatalytic reaction mechanism of MB and MO in compound **1.**

in the MOFs [33–35]. Wang and coworkers reported that series MOFs possessed nearly identical optical energy gaps, but showed different degradation efficiency on organic dyes, implying MOFs should be treated as molecular catalysts rather than as typical semiconductors [3,4,17,35]. Therefore, a possible mechanism can be proposed to clarify the degradation of organic dyes in the presence of **1** as photocatalyst [3], as illustrated in Fig. 8. In order to confirm the proposed mechanism as listed in Fig. 8, trapping experiments of radicals were applied to detect the main oxidative species in the photocatalytic process [31]. The results revealed that the addition of 1 mM isopropanol (IPA) as radical scavenger greatly inhibited the degradation efficiencies of MO (decrease from 94.1% without IPA to 49.7% with IPA as scavenger) and MB (decrease from 91.7 to 85.1%) under UV light irradiation, which suggested that oxygenous radicals were the main active species in this system.

3.6. Stability

The stability of compound **1** was checked by circulating runs in the photocatalytic degradation of MB under the same conditions. The PXRD diffraction patterns of the used photocatalyst were found be similar to that of the as-prepared photocatalyst before reactions, as illustrated in Fig. 3, indicating that there is no noticeable change in the crystallographic structure of the photocatalyst after five runs reactions. These results demonstrated that the compound **1** photocatalyst was stable under the experimental reaction conditions, and could be used circularly five runs.

4. Conclusion

In summary, compound **1** appears to be a photocatalyst to achieve preferential degradation of typical organic dyes (MB and MO) used in textile industries. And the results revealed that compound **1** exhibited efficient degradation of individual MO and MB, and preferential degradation of MO in the MO/MB mixture in short time. The effect of initial pH test on photocatalytic degradation that **1** has great stability in strong acid and alkali. Additionally, possible photocatalytic mechanism was also proposed and discussed, which was also confirmed by trapping experiments of radicals with the addition of isopropanol as radical scavenger. Further researches should be carried out to clarify the photocatalytic activities on other organic pollutants.

Acknowledgments

We thank the financial support from National Natural Science Foundation of China (5178013), the Beijing Natural Science Foundation & Scientific Research Key Program of Beijing Municipal Commission of Education (KZ201410016018), the Training Program Foundation for the Beijing Municipal Excellent Talents (2013D005017000004), the Importation & Development of High-Caliber Talents Project of Beijing Municipal Institutions (CIT&CD201404076), Special Fund for Cultivation and Development Project of the Scientific and Technical Innovation Base (Z141109004414087).

References

[1] C.-C. Wang, J.-R. Li, X.-L. Lv, Y.-Q. Zhang, G. Guo, Photocatalytic organic pollutants degradation in metal–organic frameworks, Energy Environ. Sci. 7 (2014) 2831–2867.
[2] H.-C. Zhou, J.R. Long, O.M. Yaghi, Introduction to metal–organic frameworks, Chem. Rev. 112 (2012) 673–674.
[3] C.-C. Wang, H.-P. Jing, P. Wang, S.-J. Gao, Series metal–organic frameworks constructed from 1,10-phenanthroline and 3,3′,4,4′-biphenyltetracarboxylic acid: Hydrothermal synthesis, luminescence and photocatalytic properties, J. Mol. Struct. 1080 (2015) 44–51.
[4] C.-C. Wang, H.-P. Jing, P. Wang, Three silver-based complexes constructed from organic carboxylic acid and 4,4′-bipyridine-like ligands: Syntheses, structures and photocatalytic properties, J. Mol. Struct. 1074 (2014) 92–99.
[5] C.-C. Wang, G.-L. Guo, P. Wang, Two sodium and lanthanide(III) MOFs based on oxalate and V-shaped 4,4′-oxybis (benzoate) ligands: Hydrothermal synthesis, crystal structure, and luminescence properties, J. Mol. Struct. 1032 (2013) 93–99.
[6] C.-C. Wang, Z. Wang, F. Gu, G. Guo, Three novel lanthanide MOFs constructed from 1,3-benzenedicarboxylic acid and 1,10-phenanthroline: Hydrothermal synthesis, crystal structure and thermal properties, J. Mol. Struct. 1004 (2011) 39–44.
[7] J. Lee, O.K. Farha, J. Roberts, K.A. Scheidt, S.T. Nguyen, J.T. Hupp, Metal–organic framework materials as catalysts, Chem. Soc. Rev. 38 (2009) 1450–1459.
[8] C.-C. Wang, Y.-Q. Zhang, J. Li, P. Wang, Photocatalytic CO2 reduction in metal–organic frameworks: A mini review, J. Mol. Struct. 1083 (2015) 127–136.
[9] J.-R. Li, R.J. Kuppler, H.-C. Zhou, Selective gas adsorption and separation in metal–organic frameworks, Chem. Soc. Rev. 38 (2009) 1477–1504.
[10] R.E. Morris, P.S. Wheatley, Gas storage in nanoporous materials, Angew. Chem. Int. Ed. 47 (2008) 4966–4981.
[11] M.P. Suh, H.J. Park, T.K. Prasad, D.-W. Lim, Hydrogen storage in metal–organic frameworks, Chem. Rev. 112 (2011) 782–835.
[12] K. Sumida, D.L. Rogow, J.A. Mason, T.M. McDonald, E.D. Bloch, Z.R. Herm, T.-H. Bae, J.R. Long, Carbon

dioxide capture in metal–organic frameworks, Chem. Rev. 112 (2011) 724–781.
[13] H. Qu, L. Qiu, X.-K. Leng, M.-M. Wang, S.-M. Lan, L.-L. Wen, D.-F. Li, Structures and photocatalytic activities of metal-organic frameworks derived from rigid aromatic dicarboxylate acids and flexible imidazole-based linkers, Inorg. Chem. Commun. 14 (2011) 1347–1351.
[14] S. Zhou, Z.-G. Kong, Q.-W. Wang, C.-B. Li, Synthesis, structure and photocatalytic property of a novel 3D (3,8)-connected metal–organic framework based on a flexible triphosphonate and a pentanuclear Cu(II) unit, Inorg. Chem. Commun. 25 (2012) 1–4.
[15] Y.-P. Wu, D.-S. Li, Y.-P. Duan, L. Bai, J. Zhao, Two new Cu(II) complexes constructed by mixed-organic tectonics: Structures, magnetic properties and photocatalytic degradation of organic dyes, Inorg. Chem. Commun. 36 (2013) 137–140.
[16] N. Wu, Y. Qin, X.-L. Wang, C. Qin, E.-B. Wang, Two layered copper–bis(triazole) assemblies with Keggin polyoxoanions as pendants: Syntheses, structures and photocatalytic properties, Inorg. Chem. Commun. 37 (2013) 174–177.
[17] H.-P. Jing, C.-C. Wang, Y.-W. Zhang, P. Wang, R. Li, Photocatalytic degradation of methylene blue in ZIF-8, RSC Adv. 4 (2014) 54454–54462.
[18] A. Nezamzadeh-Ejhieh, M. Bahrami, Investigation of the photocatalytic activity of supported ZnO–TiO2 on clinoptilolite nano-particles towards photodegradation of wastewater-contained phenol, Desalin. Water Treat. 55 (2015) 1096–1104.
[19] A. Nezamzadeh-Ejhieh, M. Khorsandi, Photodecolorization of Eriochrome Black T using NiS–P zeolite as a heterogeneous catalyst, J. Hazard. Mater. 176 (2010) 629–637.
[20] A. Nezamzadeh-Ejhieh, S. Hushmandrad, Solar photodecolorization of methylene blue by CuO/X zeolite as a heterogeneous catalyst, Appl. Catal. A: Gen. 388 (2010) 149–159.
[21] A. Nezamzadeh-Ejhieh, Z. Salimi, Heterogeneous photodegradation catalysis of o-phenylenediamine using CuO/X zeolite, Appl. Catal. A: Gen. 390 (2010) 110–118.
[22] A. Nezamzadeh-Ejhieh, E. Shahriari, Heterogeneous photodecolorization of methyl green catalyzed by Fe (II)-o-phenanthroline/zeolite Y nanocluster, Int. J. Photoenergy 2011 (2011), doi:10.1155/2011/518153.
[23] A. Nezamzadeh-Ejhieh, N. Moazzeni, Sunlight photodecolorization of a mixture of Methyl Orange and Bromocresol Green by CuS incorporated in a clinoptilolite zeolite as a heterogeneous catalyst, J. Ind. Eng. Chem. 19 (2013) 1433–1442.
[24] A. Nezamzadeh-Ejhieh, H. Zabihi-Mobarakeh, Heterogeneous photodecolorization of mixture of methylene blue and bromophenol blue using CuO-nano-clinoptilolite, J. Ind. Eng. Chem. 20 (2014) 1421–1431.
[25] A. Nezamzadeh-Ejhieh, E. Shahriari, Photocatalytic decolorization of methyl green using Fe(II)-o-phenanthroline as supported onto zeolite Y, J. Ind. Eng. Chem. 20 (2014) 2719–2726.
[26] M. Bahrami, A. Nezamzadeh-Ejhieh, Effect of the supported ZnO on clinoptilolite nano-particles in the photodecolorization of semi-real sample bromothymol blue aqueous solution, Mater. Sci. Semicond. Process. 30 (2015) 275–284.
[27] Q. Chu, G.-X. Liu, Y.-Q. Huang, X.-F. Wang, W.-Y. Sun, Syntheses, structures, and optical properties of novel zinc(II) complexes with multicarboxylate and N-donor ligands, Dalton Trans. 2007 (2007) 4302–4311.
[28] J.I. Pankove, Optical Processes in Semiconductors, second ed., Dover Publications, Mineola, NY, 2012.
[29] W. Wendlandt, H. Hecht, Reflectance Spectroscopy, Interscience, New York, NY, 1966.
[30] A. Nezamzadeh-Ejhieh, M. Karimi-Shamsabadi, Comparison of photocatalytic efficiency of supported CuO onto micro and nano particles of zeolite X in photodecolorization of Methylene blue and Methyl orange aqueous mixture, Appl. Catal. A: Gen. 477 (2014) 83–92.
[31] S. Liu, C. Liu, W. Wang, B. Cheng, J. Yu, Unique photocatalytic oxidation reactivity and selectivity of TiO_2-graphene nanocomposites, Nanoscale 4 (2012) 3193–3200.
[32] R. Huo, Y. Kuang, Z. Zhao, F. Zhang, S. Xu, Enhanced photocatalytic performances of hierarchical ZnO/ZnAl2O4 microsphere derived from layered double hydroxide precursor spray-dried microsphere, J. Colloid Interface Sci. 407 (2013) 17–21.
[33] A. Hameed, V. Gombac, T. Montini, M. Graziani, P. Fornasiero, Synthesis, characterization and photocatalytic activity of NiO–Bi_2O_3 nanocomposites, Chem. Phys. Lett. 472 (2009) 212–216.
[34] H.A. Lopez, A. Dhakshinamoorthy, B. Ferrer, P. Atienzar, M. Alvaro, H. Garcia, Photochemical response of commercial MOFs: $Al_2(BDC)_3$ and its use as active material in photovoltaic devices, J. Phys. Chem. C 115 (2011) 22200–22206.
[35] M. Nasalevich, M. van der Veen, F. Kapteijn, J. Gascon, Metal–organic frameworks as heterogeneous photocatalysts: Advantages and challenges, Cryst. Eng. Comm. 16 (2014) 4919–4926.